



Advances in Void Swelling and Helium Bubble Physics

W.G. Wolfer

September 1983

UWFDM-555

Presented at the Third Topical Meeting on Fusion Reactor Materials, Albuquerque, NM,
19-23 September 1983.

FUSION TECHNOLOGY INSTITUTE

UNIVERSITY OF WISCONSIN

MADISON WISCONSIN

"LEGAL NOTICE"

"This work was prepared by the University of Wisconsin as an account of work sponsored by the Electric Power Research Institute, Inc. ("EPRI"). Neither EPRI, members of EPRI, the University of Wisconsin, nor any person acting on behalf of either:

"a. Makes any warranty or representation, express or implied, with respect to the accuracy, completeness, or usefulness of the information contained in this report, or that the use of any information, apparatus, method, or process disclosed in this report may not infringe privately owned rights; or

"b. Assumes any liabilities with respect to the use of, or for damages resulting from the use of, any information, apparatus, method or process disclosed in this report."

DISCLAIMER

This report was prepared as an account of work sponsored by an agency of the United States Government. Neither the United States Government, nor any agency thereof, nor any of their employees, makes any warranty, express or implied, or assumes any legal liability or responsibility for the accuracy, completeness, or usefulness of any information, apparatus, product, or process disclosed, or represents that its use would not infringe privately owned rights. Reference herein to any specific commercial product, process, or service by trade name, trademark, manufacturer, or otherwise, does not necessarily constitute or imply its endorsement, recommendation, or favoring by the United States Government or any agency thereof. The views and opinions of authors expressed herein do not necessarily state or reflect those of the United States Government or any agency thereof.

Advances in Void Swelling and Helium Bubble Physics

W.G. Wolfer

Fusion Technology Institute
University of Wisconsin
1500 Engineering Drive
Madison, WI 53706

<http://fti.neep.wisc.edu>

September 1983

UWFDM-555

Presented at the Third Topical Meeting on Fusion Reactor Materials, Albuquerque, NM, 19-23 September 1983.

ADVANCES IN VOID SWELLING AND HELIUM BUBBLE PHYSICS*

W.G. WOLFER

Fusion Engineering Program, Nuclear Engineering Department, University of Wisconsin, Madison, Wisconsin 53706

The extensive experimental data base on irradiated austenitic alloys reveals that swelling as a function of dose can be divided into an initial transient period of low swelling rate, followed eventually by a rate of about 1%/dpa. Whereas the transient depends strongly on microstructure, temperature, and composition, the final rate of swelling is nearly independent of these variables. Models of void nucleation and growth are reviewed to demonstrate that they provide theoretical results which are in general agreement with the basic features of the observed swelling behavior. According to these models, the transient period comprises two regimes, one period of nucleation to obtain the void number density at a given irradiation temperature plus a period to reach parity between the dislocation and the void sink strength. The universal swelling rate eventually achieved is characterized by a state of sink parity.

1. INTRODUCTION

An extensive data base on high-fluence swelling in the austenitic alloy class has recently been accumulated, from which a general picture has emerged with the following features. At sufficiently high fluences, the rate of swelling in the austenitic alloy class appears to approach the value of about 1%/dpa. This rate seems to be nearly independent of the alloy composition, the heat treatment, cold-working, impurity content, and, within the temperature range available in breeder reactors, it is also weakly dependent on the irradiation temperature. In contrast, the transient period preceding the period of high swelling rate is strongly dependent on all the variables mentioned above. A more detailed discussion of these experimental results is presented in two companion papers.^{1,2}

Whereas in the past it was generally believed that the early microstructural evolution will determine the rate of swelling at high doses, the general trends for swelling described above invalidate this previous as-

sumption. Accordingly, it is necessary to view the ultimate swelling rate as an intrinsic property of the lattice, depending only on the basic parameters of the lattice defects but not on the microstructural evolution. This new concept has recently been invoked by Sniegowski and Wolfer³ in their explanation of the swelling resistance of ferritic steels.

What the microstructural evolution determines, however, is the time or dose required to approach the ultimate swelling rate. This period of exposure will henceforth be referred to as the transient regime. As later discussions will show, and as is indicated in Fig. 1, the transient dose is composed of several periods of increasing length. First, at the start of the irradiation, a short period elapses before the point defect concentrations reach their stationary values. Next, there is a time lag before void nucleation commences. This is followed by the nucleation period during which a quasi-stationary current of voids overcomes the nucleation barrier. This period is terminated when the void number

*The author gratefully acknowledges the support of this research by the Office of Magnetic Fusion Energy, U.S. Department of Energy, and by the Electric Power Research Institute.

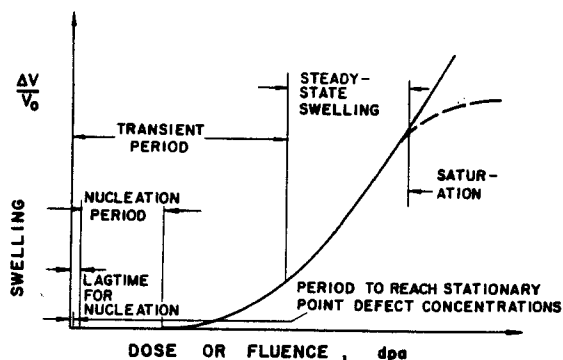


FIGURE 1
General form of swelling versus dose with the various stages involved.

density reaches its terminal value which is dependent on the temperature, microstructure, and composition of the alloy. Before the "steady-state" swelling rate can be reached, however, it is necessary for the microstructure to approach a state of parity, meaning an equalization of the dislocation and void sink strengths.

It is also indicated in Fig. 1 that the state of parity may be lost at higher doses when the dislocation sink strength drops below the void sink strength. This results then in a saturation of swelling which is often observed in ion-bombardment studies.

It will be seen in the following review that the theoretical understanding and the models developed in the past are essentially in agreement with the schematic description of swelling embodied in Fig. 1. However, when all the models are assembled into "comprehensive" computer codes, predictions of swelling vary widely.

Lacking a successful comprehensive theory at the present time, the various aspects and models involved in void nucleation and growth will be discussed separately in the following sections.

2. VOID NUCLEATION

2.1. Evolution of the Subcritical Vacancy Clusters

The time to reach stationary average concentrations of vacancies and interstitials is very short for fast-neutron irradiations and need not concern us. The time period required to establish a subcritical vacancy cluster population as a reservoir for void nuclei is also relatively short. Using a Fokker-Planck equation to describe the vacancy cluster distribution and a novel numerical path sum solution for this equation, Wehner⁴ has recently obtained detailed time-dependent cluster distributions. Figure 2 shows a typical result for the case of ion-bombardment of Ni at 500°C. The curves show the size distribution of vacancy clusters at subsequent times given in seconds. No gas was assumed to be present, and the vacancy clusters have an appreciable bias for interstitial absorption according to the capture efficiencies of Wolfer and Mansur,⁵ as well as a strong tendency to re-emit vacancies; the dislocation capture efficiency for interstitials was assumed to be equal to 1.2.

It is seen that after about 100 seconds or a dose of only 0.1 dpa, the vacancy cluster size distribution in the subcritical range has reached a quasi-stationary form. It maintains this form as long as the monovacancy concentration remains constant. With increasing dose, only the supercritical size distribution will evolve further.

The time to reach a quasi-stationary subcritical size distribution and also a constant rate of void nucleation is referred to as the incubation time, lag or delay time in nucleation theory. Figure 3 shows this time⁶ for irradiation of Ni at a dose rate of 10^{-6} dpa/s. The upper curve is for the nucleation of bare voids whereas the lower curves are for voids with segregation shells whose lattice

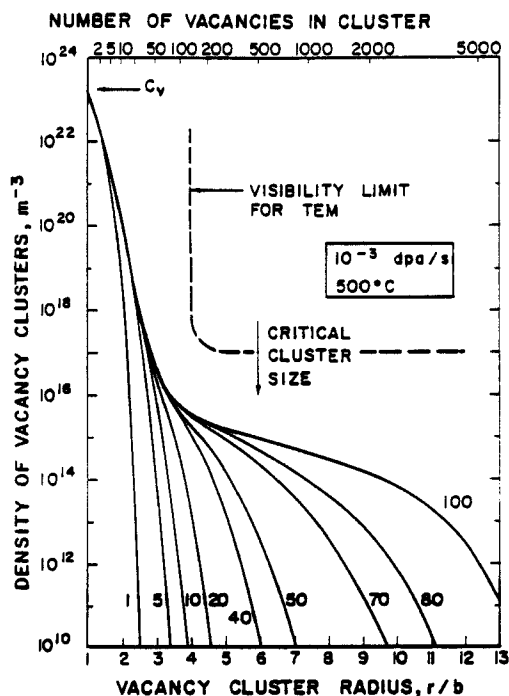


FIGURE 2

Evolution of the subcritical vacancy cluster distribution after various times indicated in seconds.

parameter differs from the value in the matrix by the amount indicated. Steady-state nucleation of bare voids commences when a dose on the order of 0.1 dpa is reached, but this dose is significantly shortened when segregation accompanies void nucleation. In any case, however, this lag or delay time is not to be confused with the much larger transient period for swelling.

2.2. Factors Influencing Void Nucleation Other Than Gases

The transient is partly determined by the void nucleation rate itself, as can be easily demonstrated with the results⁶ of Fig. 4. The void nucleation rates are shown as a function of temperature for nickel irradiated at 10^{-6}

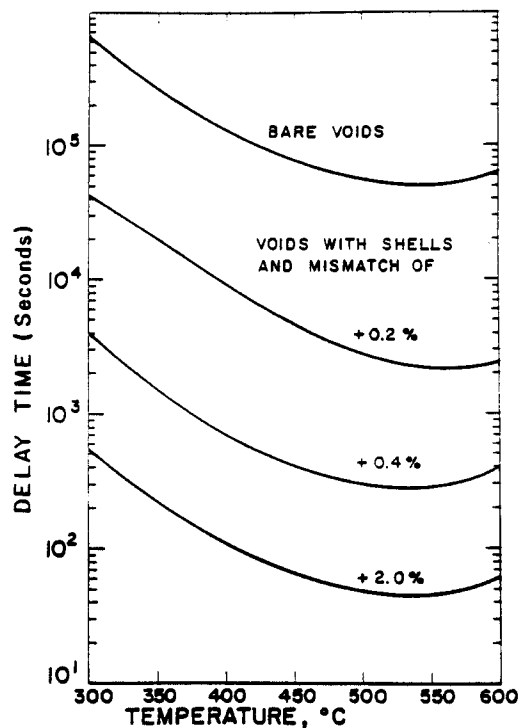


FIGURE 3

Delay time to achieve a steady-state void nucleation rate for irradiation of nickel at 10^{-6} dpa/s and for segregation shells with positive lattice parameter mismatch.

dpa/s. In order to obtain a void number density of 10^{21} m^{-3} at 450°C , 10^9 dpa would be required to nucleate this number of bare voids. However, only 0.2 dpa is needed to nucleate 10^{21} m^{-3} voids with a segregation shell of 0.2% lattice parameter mismatch. In the latter case, the corresponding delay dose is only 0.005 dpa. For the cases illustrated in Figs. 3 and 4, a dislocation bias factor ratio of 1.25 was assumed.

In the light of more recent work³ it appears that this bias factor ratio may be significantly larger than 1.25. As Fig. 5

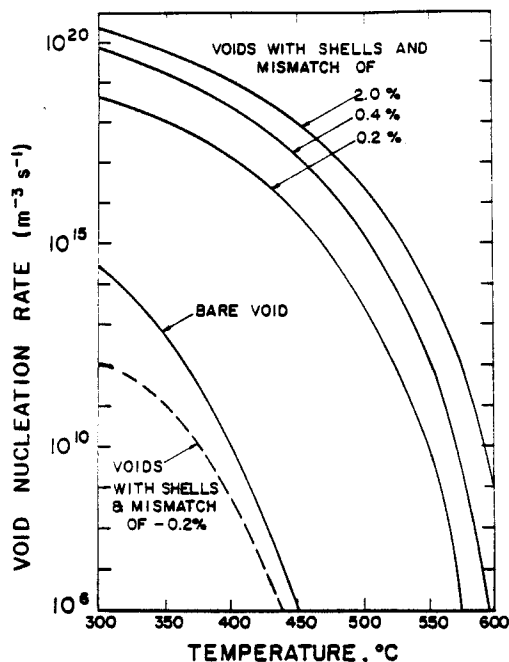


FIGURE 4
Void nucleation rates for nickel irradiation at 10^{-6} dpa/s.

shows, bare void nucleation increases dramatically with the bias factor ratio. When compared with the nucleation rate of coated voids it is seen that segregation need not be invoked as a prerequisite for void nucleation when the dislocation bias factor ratio is about 1.5 or larger. It should be noted that it is in fact the average bias factor ratio which controls the nucleation rate, i.e. an appropriately weighted average for all sinks, dislocation, loops, voids already present, etc. As more voids nucleate and grow, they contribute more to this average bias factor ratio, and it starts to decline. Together with the rising sink strength this leads eventually to a termination of void nucleation. The dependence of the void nucleation

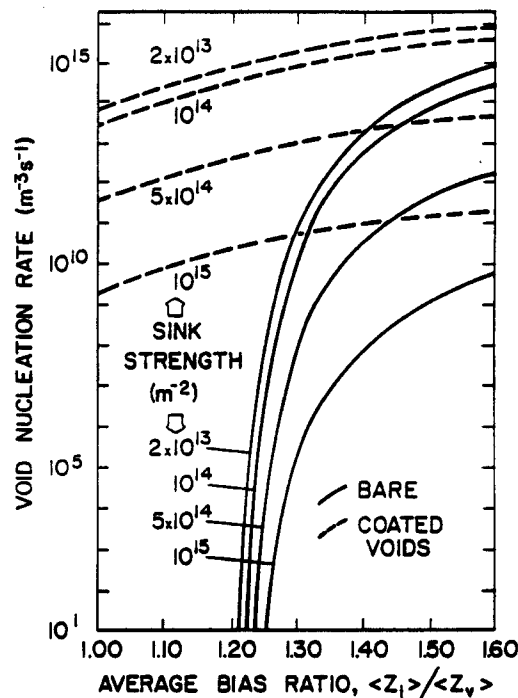


FIGURE 5
Void nucleation rates for nickel irradiated at 500°C and 10^{-6} dpa/s, assuming different average bias factor ratios. Segregation is assumed to cause a lattice parameter mismatch of 0.4%.

rate on the sink strength, as shown in Fig. 5, can also serve as an explanation for the long transient period in 20% CW type 316 stainless steel as compared to solution annealed steel.

Figure 6 illustrates the evolution of the dislocation density in these two microstructures of 316 stainless steel.⁷ For 20% CW 316, the dislocation density rapidly reaches a saturation value around $5 \times 10^{14} \text{ m}^{-2}$. In contrast, the dislocation density in the solution annealed condition rises slowly. Hence the slow rise of the dislocation density in solution annealed steels provides a favorable time window for rapid void nucleation, whereas the high dislocation density in the 20% CW

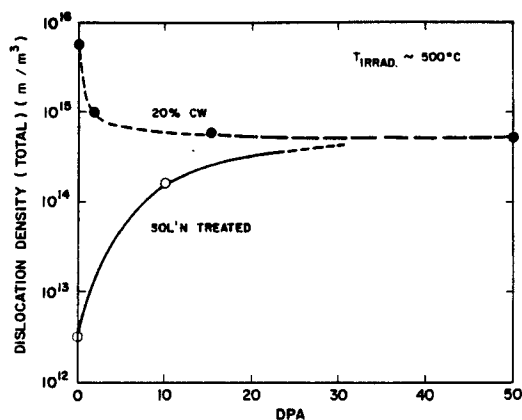


FIGURE 6
Evolution of dislocation density with fast neutron fluence in type 316 stainless steel.

steel prolongs the nucleation phase to doses close to 100 dpa.

There is another contributing factor to the rapid void nucleation in annealed materials. Due to the high supersaturation of vacancies, the divacancy concentration is also high. As shown in Fig. 7, divacancies significantly enhance the void nucleation rate⁸ relative to the case when they are not present (dashed curve) as in materials with high dislocation densities.

2.3. Effect of Inert Gases on Void Nucleation

Helium produced by transmutations has long been suspected to play a major role in void nucleation. Indeed, helium contained in small vacancy clusters can significantly reduce the vacancy reemission rate and thereby increase the nucleation rate. The results of a quantitative evaluation by Wiedersich and Hall⁹ are shown in Fig. 8. In this study, the voids are treated as neutral sinks with no bias for either interstitials or vacancies, and a surface energy of 1 J/m^2 is assumed. The dislocation bias factor ratio is chosen to be

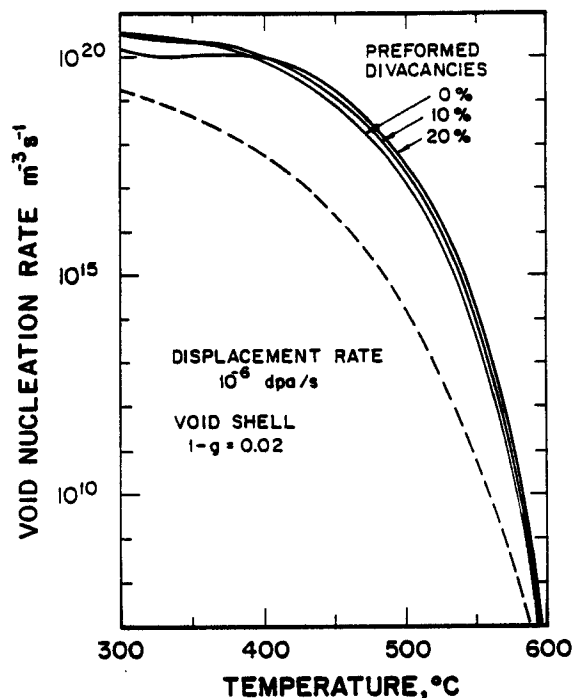


FIGURE 7
Void nucleation rates with (solid curves) and without (dashed curves) divacancies present. The assumed segregation shell is modeled as a material with a shear modulus 2% greater than the matrix. The percentage of divacancies already formed in the cascade is indicated. Dislocation density is assumed to be $2 \times 10^{13} \text{ m}^{-2}$.

1.05. Two features are noteworthy. First, small amounts of helium increase the void nucleation rate dramatically at temperatures above 400°C . Second, little enhancement is achieved for helium concentrations in excess of 10 appm. This small amount of helium is produced in a breeder reactor after 5 dpa of exposure, and after only 0.5 dpa in a future fusion reactor.

The results in Fig. 8 demonstrate the effect of the gas pressure in opposing the surface tension of small cavities when they

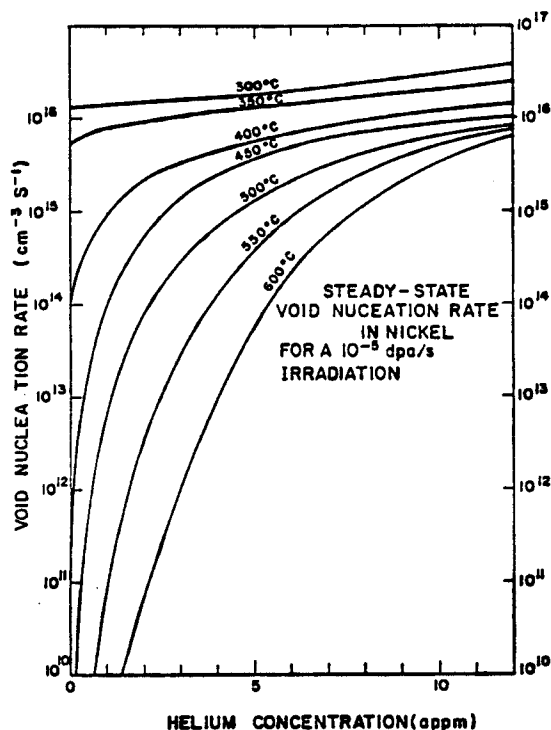


FIGURE 8
Void nucleation rate as a function of helium
content after Wiedersich and Hall.

are considered as neutral sinks. If the interstitial bias of small cavities is taken into account, however, it is found that considerably more gas is required to stabilize small cavities. In fact, an overpressure significantly larger than the surface tension must be maintained in subcritical voids, as shown in the following section on void growth.

In previous studies⁹⁻¹² on helium effects on void nucleation, the assumption is often made that a self-interstitial captured by a bubble filled with helium to a packing fraction of one will induce the emission of a helium atom. However, both the computer simulation by Wilson et al.¹⁰ and the thermodynamic analysis of Glasgow and Wolfer¹¹ show

that the reverse situation is expected; namely, additional helium atoms captured by bubbles filled already with helium will induce the emission of a self-interstitial that remains closely bound to the bubble by the image interaction. For bubbles with lower helium densities, both self-interstitial and helium interstitial emission rates are negligibly small.

2.4. Effect of Reactive Gases on Void Nucleation

Many researchers have remarked that reactive gases such as hydrogen and oxygen play a role in void nucleation although few experimental studies were specifically dedicated to investigate this particular effect. One laudable exception is the work of Glowinski and Fiche¹³ on high purity copper. Carefully out-gassed copper did not exhibit void formation up to a dose of 30 dpa whereas high purity copper not subject to high-vacuum annealing prior to irradiation did swell. The difference is presumably due to oxygen in solution which becomes chemisorbed on void surfaces and thereby reduces the surface energy and the activation barrier for void nucleation. It is interesting to note that in most void nucleation calculations a surface energy of about 1 J/m² is tacitly assumed even though this value is only about half the value measured for clean surfaces on nickel or copper.¹⁴

Chemisorption of surface-active gases such as O₂, N₂, and H₂ can indeed lower the surface energy substantially. As a particular example, Fig. 9 shows the reduction in surface energy in Ni containing various amounts of hydrogen in solution. These reductions were derived from the Langmuir-McLean isotherm and the model of Bernard and Lupis¹⁵ as described elsewhere.¹⁶ The results of Fig. 9 are of particular interest for alloys which exhibit a long nucleation period in the absence of internal hydrogen. These results suggest that

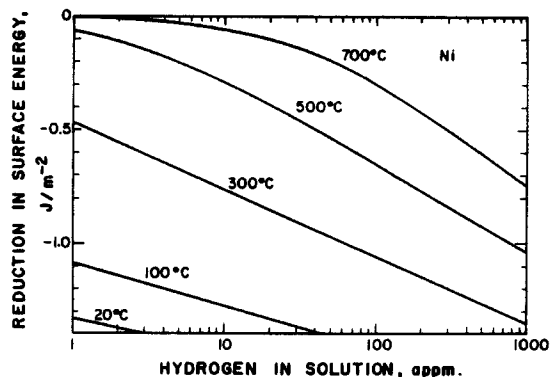


FIGURE 9
Reduction of the surface energy by chemisorbed hydrogen internally present in nickel.

the nucleation period may be shortened substantially for low temperature irradiation in a hydrogen environment.

3. VOID GROWTH

3.1. Effect of Helium on Void Growth

The formation of subcritical and even slightly supercritical vacancy clusters does not determine the onset of swelling. For small clusters, the balance of bias-driven growth and thermal vacancy emission is nearly zero. This is particularly so when the cavities are treated correctly as biased sinks rather than as neutral sinks. In this case, the net bias of a void (i.e., the difference between the bias factor ratio of dislocations and the bias factor ratio of a void of given size) changes with its radius as shown³ in Fig. 10. Large voids can indeed be considered as neutral sinks, and their net bias is simply equal to the bias factor ratio of dislocations minus one.

Above the critical radius, a void develops a positive net bias, but the initial growth rate still remains very small. In this regime of growth, the void sink strength is usually low compared to the dislocation sink strength

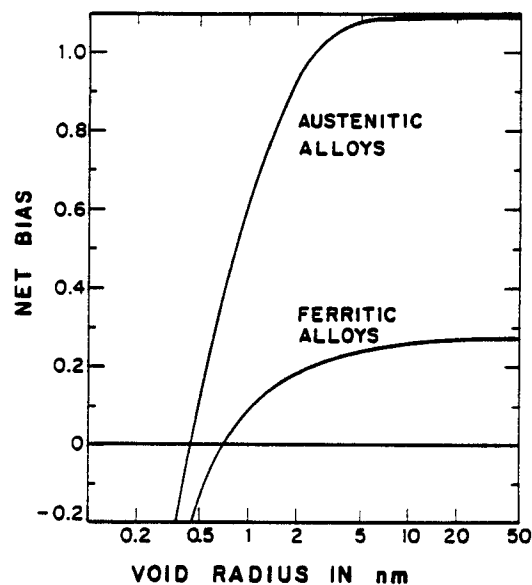


FIGURE 10
Net bias for voids in austenitic and ferritic alloys as a function of the void radius.

which further reduces its potential growth rate. Therefore, under continuous helium production, the small voids may acquire a substantial helium pressure before they enter their rapid growth phase.

In order to investigate the effect of helium on the slow growth regime, void growth calculations were performed for bare voids and various ratios of helium production to displacement rate in Ni. The number of voids was assumed to be equal to the density of voids observed in 316 stainless steels after high fluence irradiation. Both void and dislocation densities are functions of temperature as given earlier.¹⁷ The cavities were assumed to have an initial radius less than or equal to the critical radius, and helium produced during each time interval is distributed equally to all cavities. Dislocations and

void bias factors are those given in Ref. 3. The cavities can grow by either of three mechanisms, bias-driven growth, self-interstitial emission, and loop punching depending on the cavity size and gas pressure; shrinkage occurs by thermal vacancy emission. The latter process can also turn into a growth process whenever the pressure in the cavity causes the vacancy concentration in equilibrium with the cavity to drop below the average vacancy concentration in equilibrium with all the sinks.

Figure 11 shows the results of this void growth simulation for the case of helium production typical in breeder reactors. Due to the significant bias of small cavities their growth is initially so small that no appreciable swelling occurs. During the long transient period, the bias-driven growth is small and almost exactly balanced by the thermal emission rate of vacancies; only the increase in helium gas keeps the cavities expanding until bias-driven growth becomes dominant. From then on, the gas pressure in the cavities plays no further role. The onset of rapid swelling occurs at relatively high doses for a 300°C irradiation temperature because of the high density of void nuclei. At 600°C, the onset of swelling is delayed because of the large critical size the cavity must reach before bias-driven growth exceeds thermal vacancy emission.

The simulation of cavity growth in a fusion reactor environment with a helium production of 20 appm He/dpa gives the results illustrated in Fig. 12. Here, the necessary dose required to produce a sufficient amount of helium is very small, and void growth can commence almost immediately except for high irradiation temperatures. In fact, for temperatures at 700°C and above, swelling is controlled by gas-driven growth of near-equilibrium bubbles.

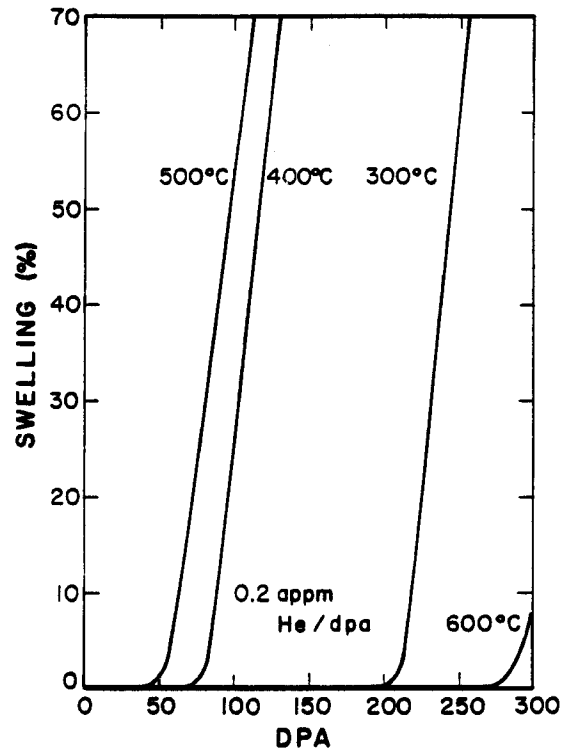


FIGURE 11
Swelling simulation after nucleation for type 316 stainless steels irradiated at 10^{-6} dpa/s under continuous helium production typical of breeders.

3.2. Effect of the Dislocation Evolution

The initial evolution of the dislocation structure is determined by a generation rate due to loop coalescence and dislocation climb and by an annihilation rate due to climb-induced recovery. When both are balanced,¹⁸ a stationary or saturation density ρ_s is reached. In type 316 stainless steels, the dose required for saturation varies between 10 to 50 dpa depending on the irradiation temperature, and the saturation density is between 2×10^{14} to 10^{15} m^{-2} depending on dose rate and heat treatment. Pure alloys tend to have low values of ρ_s , whereas high-strength alloys have higher values of the saturation dislocation density.

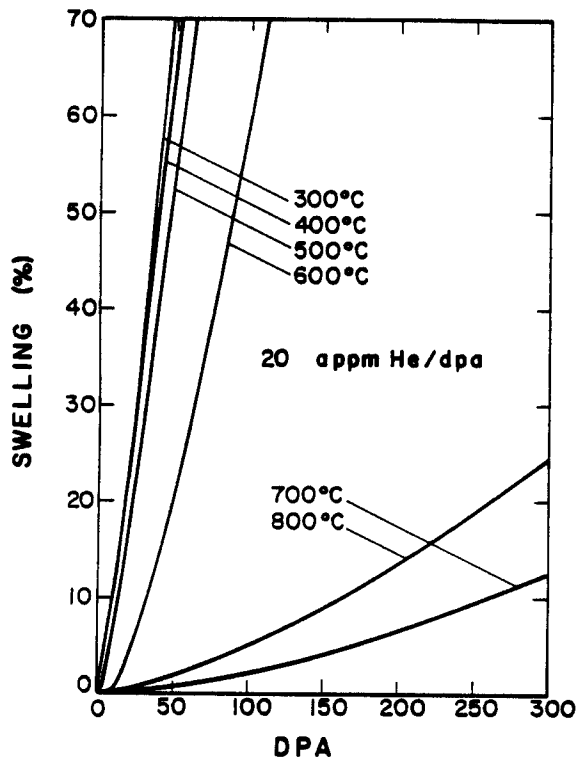


FIGURE 12

Swelling simulation after nucleation for type 316 stainless steel irradiated at 10^{-6} dpa/s under continuous helium production typical of a fusion reactor.

For a given dislocation sink strength S_d , and a given void sink strength $S_0 = 4\pi N_0 r$, the swelling rate due to bias-driven growth alone is given by^{2,3}

$$\frac{d(\frac{\Delta V}{V})}{d(dpa)} = \frac{S_0 S_d}{(S_0 + S_d)^2} 100 \beta B \left(\frac{F}{\beta P} \right). \quad (1)$$

Here, P is the displacement rate, β the fraction of point defects surviving the in-cascade recombination, and B is the net bias of large voids. Voids or bubbles with small net bias are excluded from the void sink strength as they do not yet contribute to the bias-driven growth. However, they are included in the definition of the function F . The function F/P becomes, however, nearly a constant² for temperatures between 350°C and

650°C when the total sink strength exceeds about $2 \times 10^{14} \text{ m}^{-2}$.

It is evident from Eq. (1) that a maximum in swelling rate can be achieved when parity exists between sinks of extreme bias, i.e. when $S_0 = S_d$. Since $S_0 < S_d$ in general, the rate of swelling is less than optimal but increases with dose. The universal rate of swelling of about 1%/dpa reached at high fluences in almost all austenitic alloys indicates that a state of sink parity is eventually reached and subsequently maintained to high values of swelling. This view is further reinforced by the fact that a rate of 1%/dpa is close to the maximum rate predicted according to Eq. (1) and the bias evaluation for austenitic alloys.³

In order to maintain sink parity with increasing swelling, the dislocation density must evolve further rather than remain at the saturation value ρ_s . Such a post-saturation evolution can be easily rationalized on the following basis. For large void swelling, the dislocation density may be considered as being composed of two components. One, the matrix dislocation density ρ_m consists of dislocations and loops not intersected by voids. We may assume that this density is equal to ρ_s times the volume fraction occupied by bulk metal, i.e.

$$\rho_m = \rho_s \left\{ 1 - \frac{4\pi}{3} N_0 (r + d)^3 \right\} \quad (2)$$

where d is the width of a zone around the void in which dislocations no longer act as biased sinks because of their proximity to the void surface. The other contribution comes from all those dislocations which are intersecting voids. If $2R$ is the average distance between voids and n the number of dislocation segments terminating on the void surface, then the additional density of dislocations is

$$\rho_v = \frac{n(R - r - d)}{\left(\frac{4\pi}{3} R^3\right)} \quad (3)$$

Note that $\Delta V/V = (r/R)^3$. (4)

If each void is connected by one dislocation segment to its nearest neighbors, then n may be assumed to be close to 12. Using Eq. (4) and the definitions for the void sink strength $S_o = 4\pi N_o r$ and the dislocation sink strength $S_d \equiv \rho_m + \rho_s$, Eq. (1) can be written as a differential equation for the swelling rate. Simple numerical integration then gives the swelling as a function of the dose. The parameters (βB) are chosen to give a maximum swelling rate of 1%/dpa.

Figure 13 shows the results obtained from this simple model for the case of $d = 0$. Note that $\Delta V/V_o = (\Delta V/V)/[1 - \Delta V/V]$ is plotted as this is the measure of swelling obtained from immersion density measurements. The various curves correspond to different values of the parameter $\rho_s R^2/3$. Large values of this parameter represent microstructures with either a high dislocation saturation density, a low void number density (and therefore a large average distance R between voids), or both. For these microstructures, sink parity is reached only after long irradiation exposures, giving rise to a much expanded transient period for swelling. On the other hand, for low values of $\rho_s R^2/3$, typical of microstructures with low dislocation densities and high void number densities, swelling proceeds after nucleation immediately at the maximum rate.

The parameter d is at the present time not well defined, but it may perhaps be interpreted as the distance between jogs along the edge dislocation. In pure materials with few impurities, this parameter could be large. Furthermore, in materials with low friction stress for dislocation glide, a denuded zone may exist around voids which may be characterized by a large parameter d .

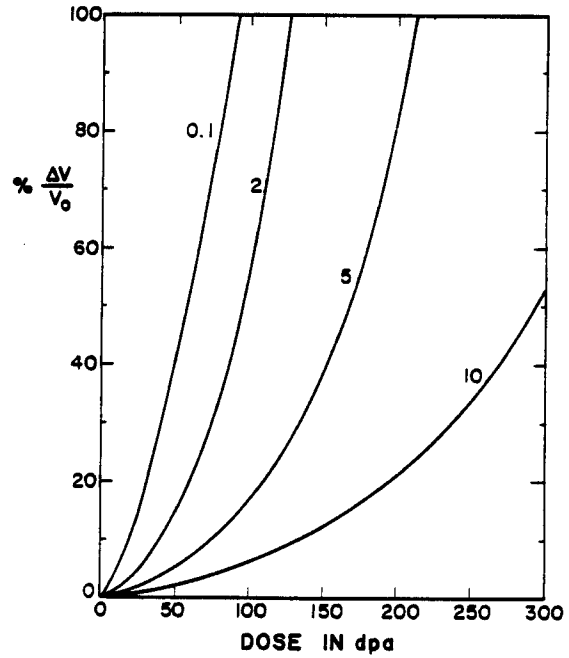


FIGURE 13
Swelling simulation after nucleation with evolving dislocation density for zero denuding.

For two choices of d/R , the results in Fig. 14 show that saturation of swelling does occur as the effective dislocation sink strength vanishes. The simple dislocation model presented here may provide some guidance in the explanation of swelling saturation observed in ion-bombardment experiments.¹⁹

4. DISCUSSION AND CONCLUSIONS

The theoretical models which have been developed in the past can indeed explain the general form of the swelling-dose relationship illustrated in Fig. 1. The important factors which determine the extent of the transient period are the period of continuous void nucleation and the subsequent growth period of voids to reach sink parity with the saturation dislocation density. The period to establish this saturation density overlaps the period of continuous void nucleation. A crucial time window exists for annealed material in which

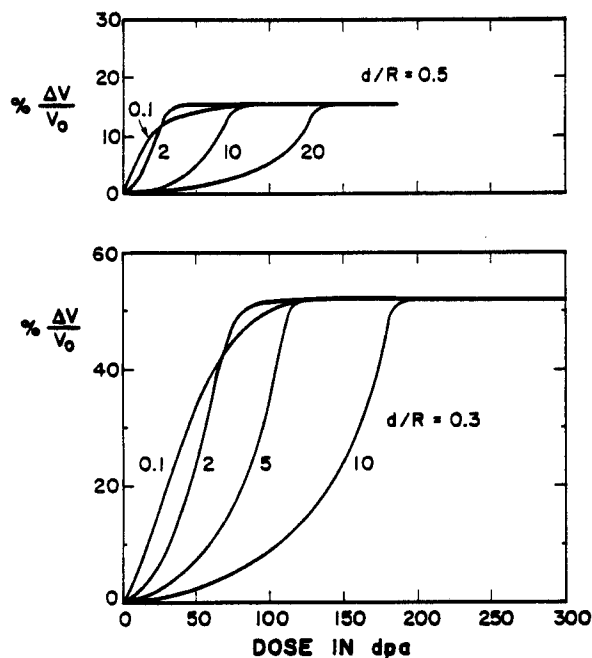


FIGURE 14
Swelling simulation after nucleation with evolving dislocation density and finite denuding.

the dislocation density remains low for rapid void nucleation to occur. In contrast, such a time window does not exist for cold-worked materials, and void nucleation proceeds at a much reduced rate. Hence, the transient period for cold-worked materials is significantly longer than for the corresponding annealed materials.

Following the termination of void nucleation, the swelling transient period continues until the void sink strength becomes about equal to the dislocation sink strength. Once sink parity is reached, the rate of swelling is mainly determined by the net bias for large voids and by the survival fraction of point defects produced in the cascade. Microstructure and temperature exert a minor influence on the "steady-state" swelling rate.

The rate of void nucleation is very sensi-

tive to segregation, to the presence of surface-active impurities, to the gas pressure produced at high temperatures in void nuclei, and to the bias exerted by the dislocation structure. Although the action of each factor is in principle understood, the synergistic action of all the factors is not. As a result, it is not yet possible to predict the length of the nucleation period or the final number of voids nucleated. For the same reason it is also not yet possible to evaluate the period required to reach sink parity.

Three aspects must be considered when evaluating the effect of helium on void swelling: the increase in void nucleation rate particularly at high temperature; the spontaneous formation of overpressurized bubbles which remain largely dormant until they grow by further helium capture to a size where their interstitial bias becomes small; and the growth of near-equilibrium bubbles at temperatures which are, however, above the range of practical interest.

In recognition of these helium effects, three strategies are suggested for alloy development with applications to future fusion reactors.

One is to develop alloys with long transient periods by producing either a high dislocation density or a high cavity density but not both. For the first case, the onset of swelling is delayed because of the longer time required to reach sink parity. In the second case, the microstructure is already past the stage of parity and evolving towards swelling saturation. This strategy can only succeed if the high density of cavities can be maintained, i.e. if coalescence and radiation-induced resolution can be prevented.

The third strategy, however, is to develop materials with a low intrinsic net bias in addition to a high dislocation density. This strategy appears to be the most promising for

the long-range development of structural materials for fusion applications.

REFERENCES

1. F.A. Garner, "Recent Insights on the Swelling and Creep of Irradiated Austenitic Alloys," Proc. 3rd Top. Mtg. on Fusion Reactor Materials, Albuquerque, NM, Sept. 19-22, 1983.
2. F.A. Garner, W.G. Wolfer, "Factors Which Determine the Swelling Behavior of Austenitic Steels," *ibid.*, 1983.
3. J.J. Sniegowski, W.G. Wolfer, "On the Physical Basis for the Swelling Resistance of Ferritic Steels," Proc. Top. Conf. on Ferritic Alloys for Use in Nuclear Energy Technologies, Snowbird, UT, June 1983, in print.
4. M.F. Wehner, Doctoral Thesis, University of Wisconsin, August 1983.
5. W.G. Wolfer, L.K. Mansur, J. Nucl. Matls. 91 (1980) 265.
6. A. Si-Ahmed, W.G. Wolfer, ASTM STP 782 (1982) 1008.
7. H.R. Brager, F.A. Garner, E.R. Gilbert, J.E. Flinn, W.G. Wolfer, in "Radiation Effects in Breeder Reactor Structural Materials," Eds. M.L. Bleiberg and J.W. Bennett, AIME, 1977, p. 727.
8. W.G. Wolfer, A. Si-Ahmed, Phil. Mag. A46 (1982) 723.
9. H. Wiedersich, B.O. Hall, J. Nucl. Matls. 66 (1977) 187.
10. W.D. Wilson, M.I. Baskes, C.L. Bisson, Phys. Rev. B13 (1976) 2470.
11. B.B. Glasgow, W.G. Wolfer, "Comparison of Mechanisms for Cavity Growth by Athermal and Thermal Processes," Proc. 3rd Top. Mtg. on Fusion Reactor Materials, Albuquerque, NM, Sept. 19-22, 1983.
12. N.M. Ghoniem, S. Sharafat, J.M. Williams, L.K. Mansur, J. Nucl. Matls. 117 (1983) 96.
13. L.D. Glowinski, C. Fiche, J. Nucl. Matls. 61 (1976) 22; 61 (1976) 29.
14. L.E. Murr, Interfacial Phenomena in Metals and Alloys (Addison-Wesley Publ. Comp., Reading, 1975), p. 124-125.
15. G. Bernard, C.H.P. Lupis, Surface Science 42 (1974) 61.
16. R.H. Jones, W.G. Wolfer, "Modeling Crack Growth Processes in Fusion Reactor Materials," Proc. 3rd Top. Mtg. on Fusion Reactor Materials, Albuquerque, NM, Sept. 19-22, 1983.
17. B.B. Glasgow, A. Si-Ahmed, W.G. Wolfer, F.A. Garner, J. Nucl. Matls. 103 & 104 (1981) 981.
18. F.A. Garner, W.G. Wolfer, ASTM STP 782 (1982) 1073.
19. F.A. Garner, J. Nucl. Matls. 117 (1983) 177.